

Ultra-high frequency photoconductivity decay in GaAs/Ge/GaAs double heterostructure grown by molecular beam epitaxy

M. K. Hudait, Y. Zhu, S. W. Johnston, D. Maurya, S. Priya et al.

Citation: *Appl. Phys. Lett.* **102**, 093119 (2013); doi: 10.1063/1.4794984

View online: <http://dx.doi.org/10.1063/1.4794984>

View Table of Contents: <http://apl.aip.org/resource/1/APPLAB/v102/i9>

Published by the [American Institute of Physics](#).

Related Articles

Spectral distribution of excitation-dependent recombination rate in an In_{0.13}Ga_{0.87}N epilayer

J. Appl. Phys. **113**, 103701 (2013)

Generalized model of the dielectric function of AlInGaP alloys

J. Appl. Phys. **113**, 093103 (2013)

Correlations between the morphology and emission properties of trench defects in InGaN/GaN quantum wells

J. Appl. Phys. **113**, 073505 (2013)

Optical characterization of free electron concentration in heteroepitaxial InN layers using Fourier transform infrared spectroscopy and a 2×2 transfer-matrix algebra

J. Appl. Phys. **113**, 073502 (2013)

Influence of structural anisotropy to anisotropic electron mobility in a-plane InN

Appl. Phys. Lett. **102**, 061904 (2013)

Additional information on *Appl. Phys. Lett.*

Journal Homepage: <http://apl.aip.org/>

Journal Information: http://apl.aip.org/about/about_the_journal

Top downloads: http://apl.aip.org/features/most_downloaded

Information for Authors: <http://apl.aip.org/authors>

ADVERTISEMENT

JANIS Does your research require low temperatures? Contact Janis today.
Our engineers will assist you in choosing the best system for your application.



10 mK to 800 K LHe/LN₂ Cryostats
Cryocoolers Magnet Systems
Dilution Refrigerator Systems
Micro-manipulated Probe Stations

sales@janis.com www.janis.com
Click to view our product web page.

Ultra-high frequency photoconductivity decay in GaAs/Ge/GaAs double heterostructure grown by molecular beam epitaxy

M. K. Hudait,^{1,a)} Y. Zhu,¹ S. W. Johnston,² D. Maurya,³ S. Priya,³ and R. Umbel⁴

¹Bradley Department of Electrical and Computer Engineering, Virginia Tech, Blacksburg, Virginia 24061, USA

²National Renewable Energy Laboratory, Golden, Colorado 80401, USA

³Center for Energy Harvesting Materials and Systems (CEHMS), Virginia Tech, Blacksburg, Virginia 24061, USA

⁴Materials Science and Engineering, Virginia Tech, Blacksburg, Virginia 24061, USA

(Received 28 December 2012; accepted 26 February 2013; published online 8 March 2013)

GaAs/Ge/GaAs double heterostructures (DHs) were grown *in-situ* using two separate molecular beam epitaxy chambers. High-resolution x-ray rocking curve demonstrates a high-quality GaAs/Ge/GaAs heterostructure by observing Pendellösung oscillations. The kinetics of the carrier recombination in Ge/GaAs DHs were investigated using photoconductivity decay measurements by the incidence excitation from the front and back side of 15 nm GaAs/100 nm Ge/0.5 μm GaAs/(100)GaAs substrate structure. High-minority carrier lifetimes of 1.06-1.17 μs were measured when excited from the front or from the back of the Ge epitaxial layer, suggests equivalent interface quality of GaAs/Ge and Ge/GaAs. Wavelength-dependent minority carrier recombination properties are explained by the wavelength-dependent absorption coefficient of Ge. © 2013 American Institute of Physics. [<http://dx.doi.org/10.1063/1.4794984>]

Germanium has received significant attention for low-cost and high-density near infra-red detection,¹⁻³ template for heteroepitaxy of GaAs on Si for laser and solar cells,⁴⁻⁶ multi-junction solar cells,⁷ tunnel transistors,⁸ and high hole mobility p-channel material for next generation low-power metal-oxide field effect transistors on Si.⁹ In addition, high-quality Ge/GaAs heterostructure opens up the possibility of heterogeneous integration of photonic devices in the 1.3-1.5 μm range. Moreover, Ge epitaxial film on a large bandgap GaAs material is of immense interest due to lattice-match (mismatch $\sim 0.07\%$), which ensures larger critical thickness, lower defect density, and strain-free Ge epitaxial film. To obtain the level of material quality necessary for minority carrier device applications,^{1-7,10-12} it is necessary to grow defect-free GaAs/Ge/GaAs double heterostructures (DHs) with high minority carrier lifetime and thin top GaAs layer on Ge that can be used as interface passivation layer for integration of high-k dielectric in order to achieve Ge-based CMOS logic. Recently, minority carrier lifetimes in bulk Ge,¹³⁻¹⁵ Ge on GaAs,¹⁶ and Ge on Si¹⁷ were studied by several researchers since the carrier lifetime is one of the most important semiconductor parameters that is sensitive to the structure, density of crystal defects, and doping density in the semiconductor. The important technical challenge in achieving desired characteristics is the minimization and controlling of antiphase domains (APDs) due to polar-on-nonpolar epitaxy of GaAs on Ge. In order to achieve the APD-free GaAs layer on Ge substrate, various growth processes have been developed that include migration enhanced epitaxy (MEE), thermal cycle annealing, and use of substrate offcut. Although, high-quality GaAs/Ge/GaAs DHs have been reported by several researchers¹⁸⁻²⁴ including our own results,^{25,26} there have been no reports on the minority

carrier lifetime and carrier recombination kinetics of molecular beam epitaxy (MBE) grown GaAs/Ge/GaAs heterostructure, and this information is necessary to identify carrier loss mechanisms at each heterointerface. This investigation on MBE-grown lattice-matched GaAs/Ge/GaAs heterostructures will assist further optimization through fundamental understanding of the processes controlling the loss. *This letter provides significant advancement in understanding of GaAs/Ge/GaAs heterostructures grown by MBE. High minority carrier lifetimes are observed for Ge layer using contactless photoconductivity decay (PCD) response since photoluminescence decay measurements are not useful in obtaining minority carrier lifetime in Ge due to indirect-gap material.*

The GaAs/Ge/GaAs double heterostructures were grown by an *in-situ* growth process on 6° offcut (100) towards the [110] direction epi-ready semi-insulating GaAs substrates using separate solid source MBE growth chambers for Ge and III-V materials, connected *via* ultra-high vacuum transfer chamber. Substrate oxide desorption was done at $\sim 680^\circ\text{C}$ under an arsenic overpressure of $\sim 1 \times 10^{-5}$ Torr in an III-V MBE chamber. During the substrate oxide desorption, GaAs layer growth, and the Ge layer after growth, reflection high energy electron diffraction (RHEED) patterns were recorded for each step of the growth process. An initial 0.5 μm thick undoped GaAs buffer layer was then deposited on GaAs substrate to generate a smooth surface at 650°C , under a stabilized As₂ flux prior to transferring GaAs wafer to the Ge MBE chamber with base pressure of 6×10^{-11} Torr for Ge epilayer growth. During the Ge epilayer growth, the chamber pressure was $\sim 2.5 \times 10^{-8}$ Torr. The growth rate and the growth temperature of Ge layer studied here was 0.07 $\text{\AA}/\text{s}$ and 400°C , as determined by triple axis x-ray diffraction from Pendellösung thickness fringes, and further confirmed by cross-sectional transmission electron microscopy (TEM). After the growth of Ge epitaxial layer, the growth temperature was carefully

^{a)}Author to whom correspondence should be addressed. E-mail: mantu.hudait@vt.edu. Tel.: (540) 231-6663. Fax: (540) 231-3362.

reduced to about 50 °C, and then substrate was transferred to III-V MBE chamber for subsequent GaAs layer growth to complete the entire GaAs/Ge/(100)GaAs double heterostructure. The thickness of the undoped epitaxial Ge layer was about 100 nm and it was p-type ($\sim 1 \times 10^{17} \text{ cm}^{-3}$). Migration enhanced epitaxy with As_2 pre-layer was used for the subsequent GaAs growth on Ge epilayer with thickness of 15 nm. The growth of upper MEE GaAs layer was carried out at $\sim 350^\circ\text{C}$ to prevent out-diffusion of Ge and the simultaneous in-diffusion of Ga and As into Ge. An As_2/Ga ratio of ~ 14 and the reduced growth rate of 0.25 \AA/s were maintained at all times. Out of 15 nm GaAs layer, 3 nm was grown at 350°C , and remaining 12 nm was grown at 500°C with the same As_2/Ga ratio and the reduced growth rate.

Epitaxial films were investigated using contact mode atomic force microscopy to reveal surface morphology. The epitaxy of GaAs/Ge/GaAs double heterostructures was confirmed using a Panalytical MRD X'Pert Pro triple axis x-ray diffraction system with a $\text{CuK}\alpha 1$ line-focused x-ray source. Ultrahigh frequency photoconductive decay (UHFPCD) measurements were made on GaAs/Ge/GaAs heterostructure at 300 K to monitor the photoconductivity decay within the Ge well in order to gain insight into the carrier recombination dynamics in GaAs/Ge/GaAs heterostructure and understand the nature of GaAs/Ge and Ge/GaAs interfaces. A range of excitation wavelength of 1000–1500 nm was used as described in the following either from the front or backside illumination. PCD lifetimes were quantified by fitting the decay curve after the optical excitation pulse was removed. Complete details of this measurement technique can be found elsewhere.²⁷

To determine the structural quality and relaxation state of the 15 nm GaAs/100 nm Ge/(100)GaAs DHs, high-resolution triple axis x-ray (004) rocking curves were recorded. Figure 1(a) shows the rocking curve from the (004) Bragg line of GaAs/Ge/GaAs DH, where the epitaxial Ge layer thickness is significantly lower than the critical layer thickness. The angular separation between the (004) diffraction peaks of Ge and GaAs resulting from the difference in lattice plane spacing along with their diffraction line profiles provides information about the interface quality of the Ge film. The peak separation between the Ge epilayer and the GaAs substrate is about 140 arcsec. The appearance of Pendellösung oscillation fringes on both sides of Ge and GaAs peaks implies the presence of parallel and very sharp heterointerface. The relaxation state of Ge layer was also measured from symmetric (004) and asymmetric (115) reflections of reciprocal space maps (RSMs) measured using triple axis x-ray diffraction, shown in Figure 1(b) and 1(c), respectively. The RSMs exhibit 2 distinct reciprocal lattice point (RLP) maxima and the peak assignments corresponding to those RLP maxima are from (i) the GaAs and (ii) the Ge epilayer. One can find from these RSMs that the thickness of the fringes as shown in Fig. 1(a) associated with a thin layer now become contour of intensity. The degree of relaxation of the Ge layer was limited to only 5%, which is expected since the critical layer thickness of Ge is about $1.8 \mu\text{m}$. The minimal relaxation and the thickness fringes confirm the high-quality GaAs/Ge/GaAs heterostructure grown by MBE.

Figure 2 shows the cross-sectional TEM micrograph of a GaAs/Ge/GaAs heterostructure. Each interface of this structure is indicated by a dashed line. There are no threading

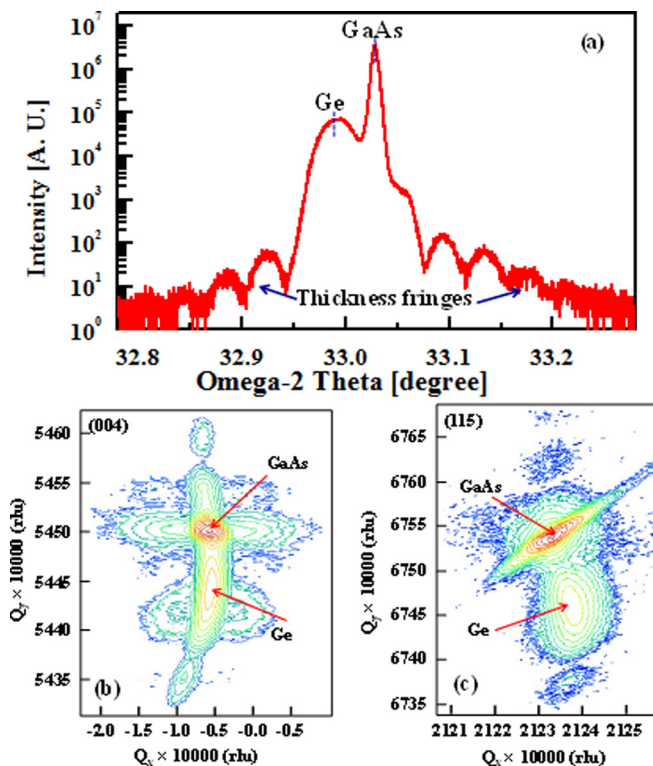


FIG. 1. (a) X-ray rocking curve from the (004) reflection of 15 nm GaAs/100 nm Ge heterostructure on (100) β GaAs substrate. The Pendellösung oscillations in the rocking curve confirm the high crystalline quality of the Ge epitaxial layer; (b) symmetric (004) and (c) asymmetric (115) reciprocal space maps of 15 nm GaAs/100 nm Ge/(001)GaAs double heterostructure. The RSMs are plotted in reciprocal space coordinates, and each epilayer peak corresponding to reciprocal lattice point is indicated in this figure.

dislocations observed in this structure, as expected since the lattice mismatch between the Ge and the GaAs is limited to only 0.07%. However, the polar-on-nonpolar growth of GaAs on Ge may produce microscopic size of APDs separated by antiphase boundaries (APBs), which can create recombination centers. As a result of these APBs, the minority carrier recombination properties can be different if the excitation is applied from the front side of the structure (GaAs on Ge) compared to the backside of the wafer (Ge/GaAs). One can

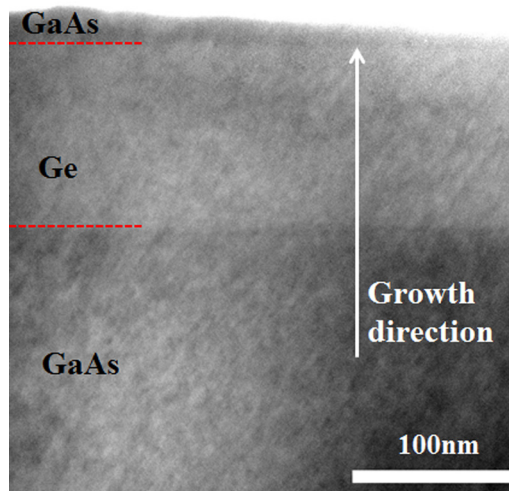


FIG. 2. Cross-sectional TEM micrograph of a GaAs/100nmGe/GaAs heterostructure. In this figure, both interfaces of GaAs/Ge and Ge/GaAs are indicated by dotted lines.

summarize from Fig. 2 that the APDs are not present at the length scales shown in the micrograph; however, the possibility of the smaller length scales of APDs is not ruled out. Although minimal, such microscopic size APDs can be expected to impact optoelectronic properties of this DH, and to investigate this possibility, UHFPCD measurements were conducted. Figures 3(a) and 3(b) show the excitation wavelength dependent PCD obtained from the GaAs/Ge/GaAs DH where the excitation was applied from the front side of the epilayer structure as well as from the back side of the GaAs substrate, respectively. The absorption coefficient of Ge varies from $2 \times 10^4 \text{ cm}^{-1}$ ($\lambda = 1000 \text{ nm}$) to $4 \times 10^3 \text{ cm}^{-1}$ ($\lambda = 1500 \text{ nm}$). As a result, the penetration depth at each wavelength is much larger than the thickness of the epitaxial Ge layer studied in this paper. By fitting the PCD data (V_{PCD}) to

$$V_{PCD} = k_1 \exp\left(-\frac{t}{\tau_{PCD}}\right), \quad (1)$$

within the low-level injection regime as indicated in these figures, PCD lifetimes (τ_{PCD}) were extracted and are shown in Fig. 4. From Fig. 4, one can find that the τ_{PCD} values were

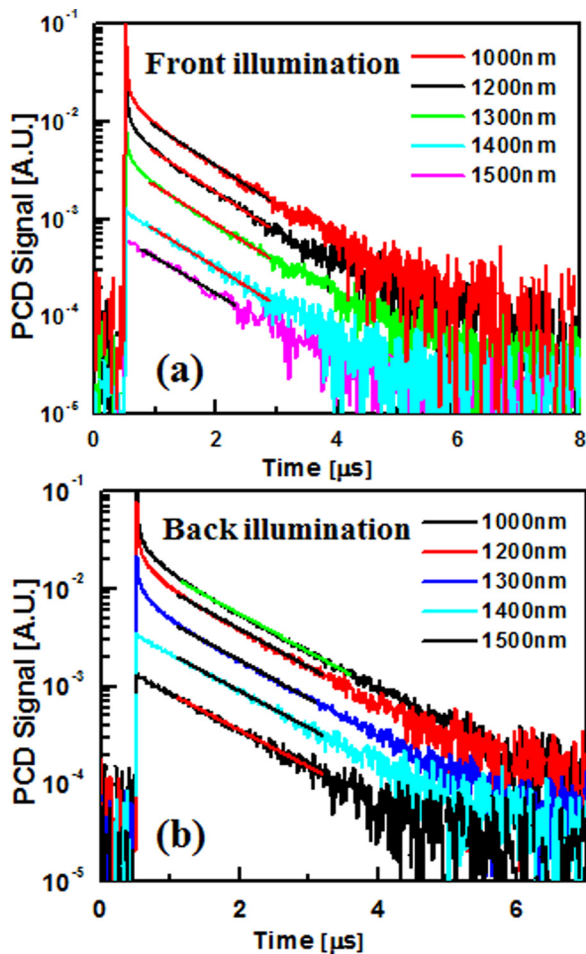


FIG. 3. Excitation wavelength dependent variations of PCD data obtained from the GaAs/Ge/GaAs DH at 300 K where the excitation was applied from the (a) front side of epilayer structure and the (b) back side of the GaAs substrate. The figure also shows the data fits to the PCD signal where the minority carrier lifetime was determined at each wavelength. The initial PCD data decreases sharply from 0 to 1 μs after excitation pulses with wavelength 1000 nm, 1100 nm, 1200 nm, and 1300 nm. The PCD data at different wavelengths were offset for clarity.

almost constant with the excitation wavelengths, reaching $\sim 1.15 \mu\text{s}$ for a 1400 nm excitation wavelength. However, Vanhellefont *et al.*²⁸ have demonstrated that the carrier lifetime in bulk Ge increases with increasing excitation level, and the possible cause for this apparent increase of lifetime compared to low excitation is due to trap filling effect. In the present study, the lifetime is almost constant with the excitation levels; suggesting that the amount of trap centers is significantly less in GaAs/Ge/GaAs heterostructure. Moreover, the PCD lifetime obtained in this work is $2.6\times$ the minority carrier lifetime measured on Ge/GaAs system¹⁶ where the lifetime is limited to 0.44 μs for an n-type Ge with residual doping concentration of 10^{18} cm^{-3} .

The impact of the interface recombination, although small is clearly evident when excitation is used for wavelength shorter than 1.3 μm . It is clearly seen from Fig. 3 that the carrier recombination does not yields a single-slope exponential decay as expected for ideal UHFPCD measurements in the wavelength range of 1000–1300 nm. The fast initial PCD decay observed is the decrease of the amplitude of the carrier decay with the excitation wavelength shorter than 1.3 μm . This may be explained by at least two phenomena: First, a high value of surface recombination velocity (S) at the upper GaAs/Ge heterointerface due to polar-on-nonpolar growth can yield multiexponential photoconductivity decay due to the higher concentration of photogenerated carriers near the upper interface that would dominate the initial part of the photoconductivity decay.²⁹ However, the similar exponential decay was observed from this heterostructure when the excitation was made from the backside of the structure, thus eliminating the possibility of the higher S at the upper GaAs/Ge interface due to large amount of APDs. This also suggests that the S is probably quite similar at these two interfaces by comparing the lifetime values shown in Fig. 4. The initial exponential decay is due to higher concentration of carriers absorbed at the surface and some degree of surface recombination, and higher injection level generates more carriers that lead to potential Auger recombination. Increasing the excitation wavelength greater than 1.3 μm , the PCD response is leading to a single-slope exponential decay.

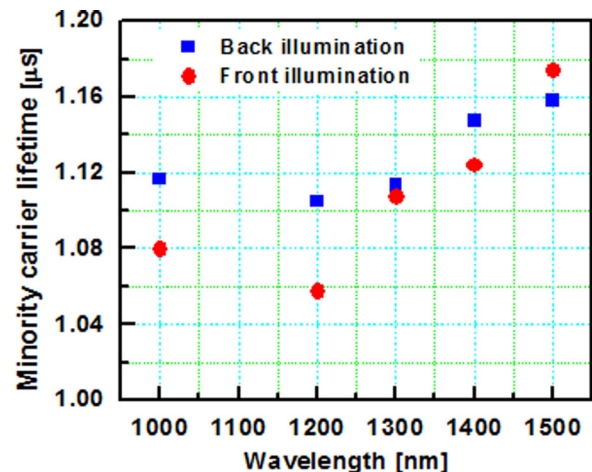


FIG. 4. Minority carrier lifetime versus excitation wavelength of GaAs/100 nmGe/GaAs double heterostructures excited from the front and back illumination. The measured minority carrier lifetime was $\sim 1.15 \mu\text{s}$ at 1400 nm wavelength.

Although the injection level was fixed at $\sim 10^{13}$ photons/cm² using the near infra-red beam from 750 nm to 2000 nm, however the injection level would need to account for absorption, thickness, surface reflection, and even perhaps lifetime for the steady-state population build-up of excess carriers. The initial fast decay is attributed due to (i) variations of injection level due to light intensity at lower wavelength or due to (ii) the interface/surface levels. Since the thickness of the epitaxial Ge layer is much lower than the penetration depth at wavelength studied in this paper, a possibility in photogenerated carrier diffusion that can occur during the transient time window²⁹ as a result of the initially nonuniform carrier generation profile that is dictated by the strong wavelength dependent absorption coefficient of the Ge layer is neglected.

In order to differentiate (if any) the nature of GaAs/Ge and Ge/GaAs heterointerfaces, the PCD data shown in Fig. 3 were re-plotted in a shorter time scale lower by 10 \times . Figures 5(a) and 5(b) compares only the initial 0-0.2 μ s PCD response of the GaAs/Ge/GaAs DH as a function of excitation wavelengths from 1000-1400 nm, where the excitation was applied from the front side and backside of the DH, respectively. In the wavelength shorter than 1300 nm (higher absorption coefficient), the PCD behavior from the upper interface (Fig. 5(a)) decreases faster compared to the bottom interface (Fig. 5(b)). This could be due to the carrier recombination at the upper GaAs/Ge interface caused by the

microscopic size of the APDs present at this interface compared to Ge/GaAs interface. However, the value of S is not enhanced by the presence of microscopic size of APDs at the GaAs/Ge heterointerface. The initial fast decay at the wavelength ≤ 1300 nm could be due to presence of interface and surface levels.

In summary, photoconductive decay measurements have been used for the optimization of the heteroepitaxy of GaAs/Ge/GaAs heterostructure by measuring the minority carrier-lifetimes as a function of excitation wavelength. The PCD lifetimes of 1.06-1.17 μ s have been demonstrated for the GaAs/Ge/GaAs double heterostructure, which are 2.6 \times higher than the reported minority carrier lifetime measured on Ge/GaAs system. In addition, outstanding GaAs/Ge interface quality is demonstrated which is comparable to the Ge/GaAs interface since the minority carrier lifetime measured by the excitation from the front GaAs/Ge and from the back Ge/GaAs were almost identical. Thus, the high-quality MBE grown GaAs/Ge/GaAs heterostructures can offer a promising path for extending the performance and application of Ge-based minority carrier and quantum well devices.

This work is supported in part by Intel Corporation.

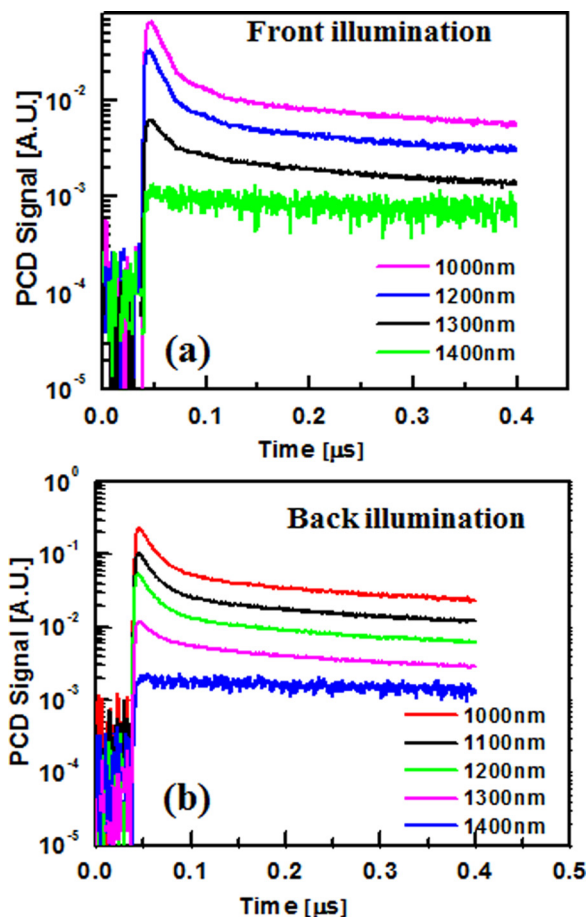


FIG. 5. Excitation wavelength dependent PCD data from Figure 3 in a shorter time scale was re-plotted where the excitation was applied from (a) the front side of epilayer structure and the (b) back side of the GaAs substrate.

¹G. Masini, L. Colace, G. Assanto, H. C. Luan, and L. C. Kimerling, *IEEE Trans. Electron Devices* **48**, 1092 (2001).

²V. Soriano, A. De Iacovo, L. Colace, A. Fabbri, L. Tortora, E. Buffagni, and G. Assanto, *Appl. Phys. Lett.* **101**, 081101 (2012).

³G. Roelkens, L. Liu, D. Liang, R. Jones, A. Fang, B. Koch, and J. Bowers, *Laser Photon. Rev.* **4**, 751 (2010).

⁴S. A. Ringel, J. A. Carlin, C. L. Andre, M. K. Hudait, M. Gonzalez, D. M. Wilt, E. B. Clark, P. Jenkins, D. Scheiman, A. Allerman, E. A. Fitzgerald, and C. W. Leitz, *Prog. Photovoltaics* **10**, 417 (2002).

⁵C. L. Andre, J. J. Boeckl, D. M. Wilt, A. J. Pitera, M. L. Lee, E. A. Fitzgerald, B. M. Keyes, and S. A. Ringel, *Appl. Phys. Lett.* **84**, 3447 (2004).

⁶O. Kwon, J. J. Boeckl, M. L. Lee, A. J. Pitera, E. A. Fitzgerald, and S. A. Ringel, *J. Appl. Phys.* **100**, 013103 (2006).

⁷R. R. King, *Nature Photon.* **2**, 284 (2008).

⁸S. Cho, I. M. Kang, T. I. Kamins, B.-G. Park, and J. S. Harris, *Appl. Phys. Lett.* **99**, 243505 (2011).

⁹R. Pillarisetty, B. Chu-Kung, S. Corcoran, G. Dewey, J. Kavalieros, H. Kennel, R. Kotlyar, V. Le, D. Lionberger, M. Metz, N. Mukherjee, J. Nah, W. Rachmady, M. Radosavljevic, U. Shah, S. Taft, H. Then, N. Zelick, and R. Chau, *Tech. Dig. - Int. Electron Devices Meet.* **2010**, 150.

¹⁰N. Jain and M. K. Hudait, *IEEE J. Photovolt.* **3**, 528 (2013).

¹¹C. L. Andre, J. A. Carlin, J. J. Boeckl, D. M. Wilt, M. A. Smith, A. J. Pitera, M. L. Lee, E. A. Fitzgerald, and S. A. Ringel, *IEEE Trans. Electron Devices* **52**, 1055 (2005).

¹²J. A. Carlin, S. A. Ringel, E. A. Fitzgerald, M. Bulsara, and B. M. Keyes, *Appl. Phys. Lett.* **76**, 1884 (2000).

¹³E. Gaubas and J. Vanhellemont, *Appl. Phys. Lett.* **89**, 142106 (2006).

¹⁴J. Vanhellemont and E. Gaubas, *ECE Trans.* **3**(4), 339 (2006).

¹⁵R. Conradt and J. Aengenheister, *Solid State Commun.* **10**, 321 (1972).

¹⁶R. Venkatasubramanian, M. L. Timmons, S. Bothra, and J. M. Borrego, *J. Cryst. Growth* **112**, 7 (1991).

¹⁷J. J. Sheng and M. S. Carroll, *Mater. Res. Soc. Symp. Proc.* **891**, 0891-EE12-09 (2005).

¹⁸Y. Bai, M. T. Bulsara, and E. A. Fitzgerald, *J. Appl. Phys.* **111**, 013502 (2012).

¹⁹E. A. Kraut, R. W. Grant, J. R. Waldrop, and S. P. Kowalczyk, *Phys. Rev. Lett.* **44**, 1620 (1980).

²⁰P. Zurcher and R. S. Bauer, *J. Vac. Sci. Technol. A* **1**, 695 (1983).

²¹W. Mönch, R. S. Bauer, H. Gant, and R. Murschall, *J. Vac. Sci. Technol.* **21**, 498 (1982).

²²H. Kroemer, K. J. Polasko, and S. C. Wright, *Appl. Phys. Lett.* **36**, 763 (1980).

- ²³G. A. Baraff, J. A. Appelbaum, and D. R. Hamann, *Phys. Rev. Lett.* **38**, 237 (1977).
- ²⁴Y.-C. Ruan and W. Y. Ching, *J. Appl. Phys.* **62**, 2885 (1987).
- ²⁵M. K. Hudait, Y. Zhu, N. Jain, S. Vijayaraghavan, A. Saha, T. Merritt, and G. A. Khodaparast, *J. Vac. Sci. Technol. B* **30**, 051205 (2012).
- ²⁶M. K. Hudait, Y. Zhu, N. Jain, and J. L. Hunter, Jr., *J. Vac. Sci. Technol. B* **31**, 011206 (2013).
- ²⁷R. K. Ahrenkiel and S. W. Johnston, *Sol. Energy Mater. Sol. Cells* **55**, 59 (1998).
- ²⁸A. Uleckas, E. Gaubas, T. Ceponis, K. Zilinskas, R. Grigonis, V. Sirutkaitis, and J. Vanhellefont, *Solid State Phenom.* **178–179**, 427 (2011).
- ²⁹Y. Lin, M. K. Hudait, S. W. Johnston, R. K. Ahrenkiel, and S. A. Ringel, *Appl. Phys. Lett.* **86**, 071908 (2005).